01 May 2007

Commensurate Phases of Gases Adsorbed on Carbon Nanotubes

Angela D. Lueking
Missouri University of Science and Technology, luekinga@mst.edu

W. Milton Cole

Recommended Citation

A. D. Lueking and W. M. Cole, "Commensurate Phases of Gases Adsorbed on Carbon Nanotubes," *Physical review B: Condensed matter and materials physics*, vol. 75, no. 19, American Physical Society (APS), May 2007.
The definitive version is available at https://doi.org/10.1103/PhysRevB.75.195425

Commensurate phases of gases adsorbed on carbon nanotubes

Angela D. Lueking[1,2] and Milton W. Cole[2,3]
[1]*Department of Energy and Geo-Environmental Engineering, Pennsylvania State University, University Park, Pennsylvania 16802, USA*
[2]*Materials Research Institute, Pennsylvania State University, University Park, Pennsylvania 16802, USA*
[3]*Department of Physics, Pennsylvania State University, University Park, Pennsylvania 16802, USA*
(Received 7 December 2006; revised manuscript received 16 January 2007; published 18 May 2007)

A study is presented of the nature of ordered phases of various gases adsorbed on an isolated carbon nanotube. Because the spacing between neighboring adsorption sites depends on the tube's radius R, the equilibrium structure of the ground state is predicted to differ from that observed on planar graphite. Results for this structure are presented for the inert gases and hydrogen as a function of R for zigzag nanotubes.

DOI: 10.1103/PhysRevB.75.195425 PACS number(s): 68.43.−h

I. INTRODUCTION

The adsorption of simple gases on graphite has been studied intensively for some 50 years.[1–5] One reason for particular interest in this system is that the strong covalent bonding and weak interplanar attraction result in porous forms of the material (needed for specific heat studies) with large exposed basal plane surfaces that are chemically inert. Gases adsorbed on such extended surfaces exhibit a wide variety of phase behaviors amenable to theoretical description as two-dimensional (2D) matter. Among these phases are nearly ideal 2D gas, liquid, and solid phases, analogous to 3D phases. For such phases, the substrate structure plays a relatively small role, so that the experimental data provide stringent tests of theories of matter in 2D. For example, the critical point behavior predicted by the Onsager solution of the 2D Ising model, which describes the liquid-vapor transition, was first confirmed by experiments with CH_4 on graphite.[6,7] In contrast to such "smooth surface" phases, commensurate phases occur for some gases, manifesting the substrate's honeycomb structure. An example of these is the $\sqrt{3}\times\sqrt{3}R30°$ phase, seen for He, Kr, and H_2, in which the admolecules localize at second-nearest-neighbor sites, above the hexagons' centers, separated by 4.26 Å.[8–10] This phase dominates the monolayer phase diagrams of these gases, persisting up to remarkably high temperatures, at which point phase transitions occur, exhibiting spectacular thermodynamic signatures of the order-disorder transition. That critical behavior is consistent with predictions based on the three-state Potts model, which is applicable because there exist three equivalent subsets of sites.[11,12]

This paper addresses analogous problems of ordered phases of gases adsorbed on carbon single-wall nanotubes (SWNTs). Research in this field has been stimulated by interest in both the fundamental science of this system and potential practical applications to gas sensing, storage, and separation technologies.[13,14] Much, but not all,[15] theoretical research concerning NT adsorption has made the simplifying assumption that the atomic structure can be neglected, resulting in a cylindrically symmetric potential energy function for adatoms, $V(r)$. Such an approximate description has been justified by a variety of arguments. One is that the corrugation of the potential, due to the atomicity, is expected to be smaller than is found on graphite.[16] Another is that uncertainties in the potential functions do not justify a detailed study of hypothetically small effects of corrugation. A third justification is based on the analogous planar case, for which the neglect of corrugation is warranted in studying those gases that exhibit nearly ideal, 2D smooth surface behavior.[17]

One should recognize that the term "commensurate" has alternative possible meanings in the present context. Here, as is customary in describing monolayer films on flat surfaces, we use the term when there exists a definite relationship (registry) between the lattice representing the substrate atoms and that of the adsorbate atoms. Such phases appear as a consequence of the periodic potential provided by the substrate. However, there can arise phases on nanotubes in which an order exists even when the potential is derived from a continuum model of the substrate, due to the azimuthal symmetry (periodic, modulo 2π) of any hypothetical phase. An example of such a phase is a periodic sequence of adsorbate rings encircling the tube. Such phases are not explored here, although they have been investigated previously by our group, and others, using cylindrically symmetric adsorption potentials.[18] The (quite common) use of such approximate potentials precludes commensurate phases of the kind discussed here.

In this paper, we focus on the role of this corrugation in producing commensurate phases of adsorbed gases on the surface of a zigzag NT. Specifically, we evaluate and compare the ground-state energies of three hypothetical phases. These are cylindrical analogs of the following hypothetical phases on graphite: the $\sqrt{3}\times\sqrt{3}R30°$ phase, the 1×1 phase, and a striped $1\times\sqrt{3}$ phase, respectively; see Fig. 1. The results of the calculations reveal which of these phases is energetically favored, as a function of the tube radius R. Our study has been carried out for the five inert gases and H_2; the phase behaviors of these gases on the basal plane surface of graphite have been explored extensively and are relatively well understood.[1–5] An analogous study of commensurate phases of K on carbon nanotubes was presented recently by Yang and Ni.[19] Their results revealed that high-density phases [e.g., a $(1\times2)R0°$ phase] exist on small-radius tubes, as will be shown below for the case of noble gases and H_2. The high-density phase shown to be stable by Yang and Ni for K adsorption to a (6,0) SWNT is equivalent to the "striped" phase considered here.

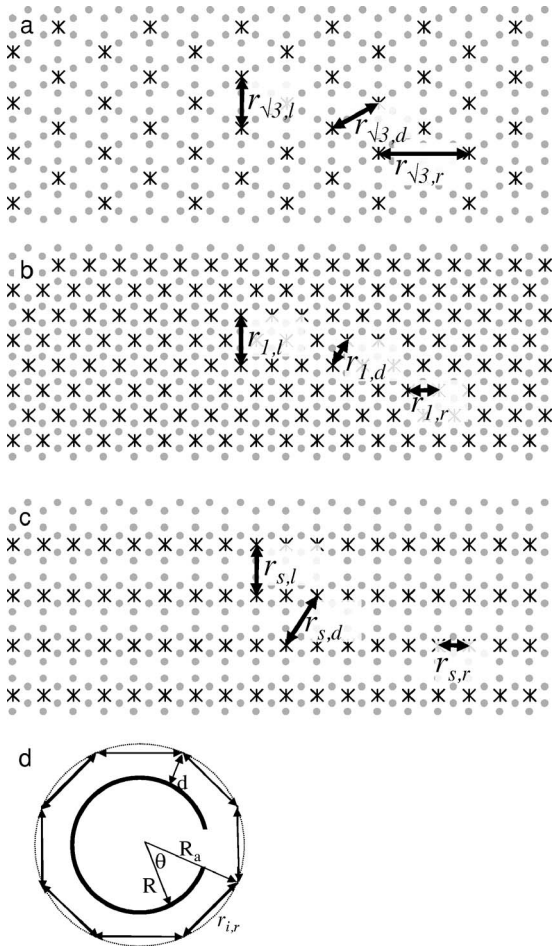

FIG. 1. Nanotube projected onto two dimensions by "unrolling" the cylindrical graphite sheet (a)–(c). Adatoms (∗) are arranged in (a) $\sqrt{3}\times\sqrt{3}R30°$ phase, (b) 1×1 phase, and (c) striped $1\times\sqrt{3}$ phase. The transverse cross-section (d) shows the relation between tube radius R, the radius of the adatom overlayer R_a, equilibrium adsorption distance d, and the radial adatom nearest-neighbor distance r_{ir}. Other nearest-neighbor distances, including diagonal r_{id} and longitudinal r_{il}, are defined in the figure. Unlike planar graphite, these various distances are not equal, due to the curvature (see text).

In the following section, we compare the energies of the three possible phases being considered. This analysis is carried out classically, a severe approximation for the more quantum gases He and H_2. This point and other qualitative concerns are explored in Secs. II and III. Section III also discusses possible experimental observation of the phases proposed here. Since quantum effects are omitted, we need only minimize the potential energy to find the equilibrium phase. Phases of higher energy per particle are metastable.

II. ANALYSIS

A. Geometrical considerations

The separations r_{ij} between nearest-neighbor adatoms are functions of the tube radius R and the equilibrium distance between the adatoms and the tube, d [defined as the distance between the nanotube cylinder and the outer adatom cylinder: see Fig. 1(d)]. The radial nearest-neighbor separation r_{ir}, involves a relatively straightforward geometrical relation. When the number of adatoms along any given cross section is equal to N, the radial separation distance r_{ir} is given by

$$r_{ir} = 2\left(\frac{Na}{2\pi} + d\right)\sin\left(\frac{\pi}{N}\right).$$

Here a is the width of a hexagon, 2.46 Å for graphene. Due to curvature, the radial nearest-neighbor separation between adatoms, r_{ir}, is not equal to the diagonal r_{id} or longitudinal r_{il} separations. The r_{il} separation is equal to the separation in graphite (i.e., 4.26 Å), while both r_{id} and r_{ir} are functions of tube radius, chirality, and equilibrium adsorption distance d. The diagonal nearest-neighbor separation is less than the radial nearest-neighbor distance. As the diagonal r_{id} is always greater than the r_{il} separation, the spacing of adatoms along the diagonal will be the limiting factor for the stability of this phase. The striped phase, which lacks nearest neighbors along the diagonal [see Fig. 1(c)], will be limited by the radial separations. These limiting nearest-neighbor interactions are plotted in Fig. 2: the relationships between gas-gas and gas-carbon separations are shown with the limiting adatom interaction indicated. The limiting adatom interaction for the $\sqrt{3}$ phase is the longitudinal distance, the limiting adatom interaction for the striped phase is the radial interaction, and the limiting interaction for the 1×1 phase is the diagonal interaction. Also shown in Fig. 2 are comparisions of these interactions with the σ parameters for the various gases in this study. One might anticipate that calculations of the adatom separations would facilitate predictions of when adatom placement in a particular configuration leads to repulsion, resulting from overlap of the hard-core diameter σ, which is greater than 2.5 Å for every gas. For example, in the case of H_2 ($\sigma_{H_2\text{-}H_2}$ is 2.928 Å), one might anticipate that, as the H_2 nearest-neighbor distance decreased to less than 2.928 Å with decreasing d, repulsion would occur due to overlap of the H_2-H_2 potentials. Similarly, as the carbon-hydrogen distance decreased to less than the $\sigma_{H_2\text{-}C}$ of 2.97 Å with decreasing d, one would expect repulsion to occur and the interaction to become energetically unfavorable. Figure 2 thus becomes an interesting geometric approximation of the regions of energetic stability. If a point representing $\{\sigma_{gC}, \sigma_{gg}\}$ falls below the line corresponding to a given phase the distances are such that repulsions can be expected. For example, for

$N=15$ helium and neon fall below the limiting line for the 1×1 phase, while H_2, Ar, and Kr fall below the limiting line for the striped phase and Xe is above the striped phase and below the line for the $\sqrt{3}$ phase [Fig. 2(a)]. Thus, by geometrical considerations alone, one may predict that for $N=15$ the 1×1 phase is the favored phase for He and Ne, striped is the favorable phase for H_2, Ar, and Kr, and $\sqrt{3}$ is the favored phase for Xe. Similarly, for $N=18$ [Fig. 2(b)], the geometrical argument predicts that 1×1 is favored for He, striped is favored for H_2 and Ar, and $\sqrt{3}$ is favored for Kr and Xe; Ne falls almost exactly on the line for the transition

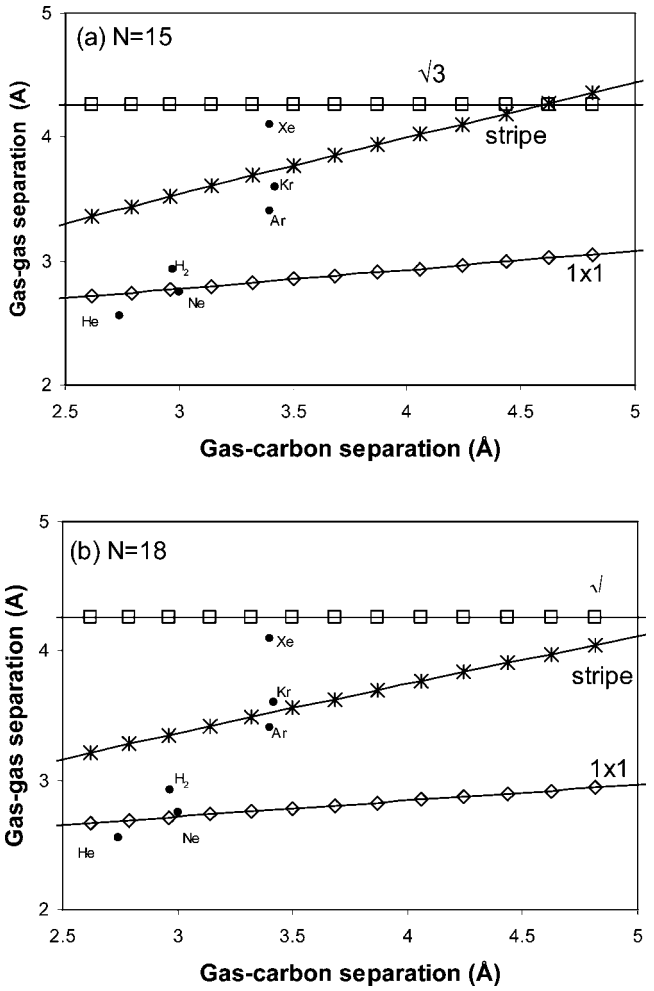

FIG. 2. Resulting gas-gas separation and gas-carbon separation as the distance between the NT and adatom is varied, for $N=15$ and $N=18$ tubes. The lines represent the limiting (shortest) distances for the various phases, as shown. Also plotted are $\{\sigma_{gC}, \sigma_{gg}\}$ for the various gases. The relative phase stability can be estimated from these curves, as discussed in the text.

between 1×1 and striped, and thus it is difficult to predict which phase is favored for Ne.

The geometrical argument does help one understand why the 1×1 phase and the (striped) $1\times\sqrt{3}$ phase do not occur for planar graphite: on the basal plane the hypothetical striped phase would involve occupation of closely spaced, nearest-neighbor sites (2.46 Å apart) and more distant second-nearest-neighbor sites (4.26 Å apart). The nearest-neighbor adatom separation in the $\sqrt{3}$ phase on planar graphite is 4.26 Å in each direction, greater than the hard-core diameter for all gases studied here. In the NT case, however, the tube's curvature results in an expansion of this distance, so that the separation between sites increases to the point where nearest neighbors attract one another. The resulting phase will be seen to have lower energy than the alternative phases in some circumstances.

This geometrical argument can be quantified in terms of the following working hypothesis: the most energetically favored phase is that for which the adatoms' nearest-neighbor separation (d_{NN}) comes *as close as possible* to the atomic diameter (σ_{gg}), but d_{NN} cannot be less than that diameter (or else hard-core overlap occurs). While a plausible conjecture, the argument is approximate, at best, because it ignores both the detailed *shapes* of the two interaction potentials and their well depths. This geometrical argument will be shown in Sec. III to be a valuable guide to predicting structure, even though it ignores the detailed energetic aspects of the full calculation.

B. Calculations of energies of various phases

In this section, we compute the ground-state energies of possible phases of gases adsorbed on nanotubes of varying radii. We have focused on zigzag tubes having chiralities $(N,0)$. Each simulation is run from $N=6$ to the N value at which the $\sqrt{3}$ phase is observed to become stable or $N=90$, whichever is less. Figures generally focus on $N=6-21$, as this sequence provides a representative grouping of such tubes, involving radii $R\approx N\times0.39$ Å, which are typical of tubes found experimentally. The restriction of this study to the zigzag case was arbitrary; however, the nearest-neighbor interactions for the zigzag NT benefit from curvature to a greater extent than for other chiralities. For example, longitudinal nearest-neighbor distance of the armchair NT is 2.46 Å, the same as for graphite. Based on the geometrical arguments discussed in Sec. II A, this suggests that a 1×1 phase in an armchair NT would not occur. A striped phase may occur, but the orientation of the adatoms would spiral around the NT rather than have transverse rings as in the case of the zigzag NT. Thus, the relative benefits from curvature transitions between phases depend on chirality, and are expected to be greatest for the zigzag NT.

Since quantum effects are omitted, we need only minimize the potential energy to find the equilibrium phase. A quantum treatment would be straightforward, in principle, for individual atoms, in the form of a band structure calculation, analogous to that carried out for planar surfaces.[20] However, the case of finite coverage would necessitate the use of more complicated methods (e.g., diffusion Monte Carlo, density functional, or quasiharmonic phonon theory methods).[21,22]

The potential energy of these various phases is computed by evaluating E, the energy per atom (molecule in the H_2 case), as a function of the distance d of the atom above the nanotube surface. This distance is assumed to be constant for all adatoms, as indicated in Fig. 1(d), omitting the unlikely possibility of superlattice overlayer phases. For each specific $(N,0)$ tube, we compute the potential energy of the three phases shown in Fig. 1, considering the energy due to both gas-gas interaction and gas-carbon interaction. The total energy is thus the sum of two terms:

$$E = E_{gg} + E_{gC}, \tag{1}$$

where E_{gg} is the gas-gas interaction, derived by summing Lennard-Jones (LJ) interactions between each adatom and its fellow adatoms, dividing by 2 to avoid double counting. E_{gC} is the energy of the adatom's interaction with the carbon atoms of the nanotube. The values used for the gas-gas LJ interaction parameters are conventional, taken from Ref. 23.

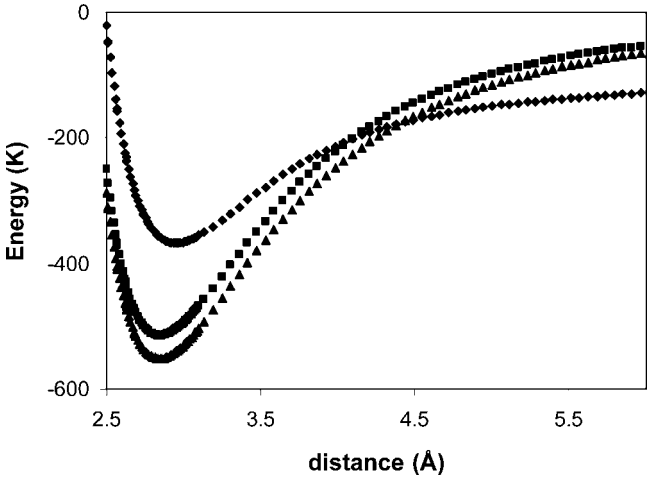

FIG. 3. Adsorption energy of H_2 as a function of distance d, for the case of an $N=18$ tube. Curves represent results for the 1×1 phase (diamonds), the $\sqrt{3}$ phase (squares), and the striped phase (triangles).

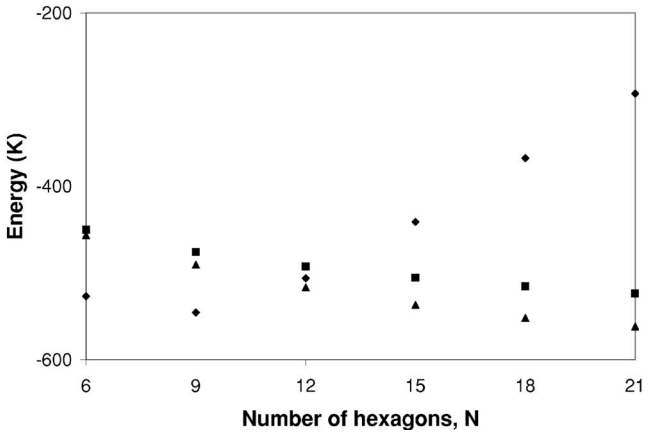

FIG. 4. Adsorption energy for H_2 as a function of N. Symbols as in Fig. 3.

The LJ parameters for the gas-gas interactions span a factor of 20 range in well depth ε and a factor of 1.6 range in value of the σ parameter. The values of the gas-carbon interaction parameters are taken from Table 2.1 of Ref. 5. Because these latter values are derived from (geometrical or arithmetic average) combining rules, their range of variation is smaller than that of the gas-gas interaction.[24]

Figure 3 presents results for the energy per molecule as a function of adsorption distance d for the case of H_2 and $N=18$ ($R\sim7.0$ Å). The relative energies of the three phases reflect the adatom separation distances: the lowest possible energy occurs for the striped phase, near the distance $d_{\min}=2.85$ Å, at which point $E=-552$ K. The $\sqrt{3}$ phase has an optimized energy $E=-515$ K, meaning that this phase is about 7% less strongly bound than the striped phase. The 1×1 phase has $E\sim-367$ K, far above the others. The increased energy of the 1×1 phase is due to repulsive contributions of H_2-H_2 interactions along the diagonal. The equilibrium distance d in this 1×1 phase (2.94 Å) is about 3% larger than that found for the other two phases (2.85 Å), a consequence of the need to reduce the mutual repulsion of the H_2-H_2 interactions along the diagonal (at the expense of the substrate attraction). A principal distinction between the two favored phases' energies arises from the intermolecular potential. For the striped phase at equilibrium, the nearest-neighbor separation is 3.44 Å, just 4% larger than the dimer's equilibrium separation, 3.29 Å, so this pair interaction is nearly optimized. In contrast, the longitudinal nearest neighbor separation of the $\sqrt{3}$ phase is much larger, 4.26 Å, than that of the other phases. The corresponding energy difference (striped vs $\sqrt{3}$) between these nearest-neighbor interactions is 23 K per molecule, a significant contribution to the 37 K energy difference between these phases.

Figure 4 presents the H_2 energies at optimal d for tubes of varying N. For small-R tubes (i.e., $N<12$), the curvature is sufficiently large that the 1×1 phase is stable. This is explained, in part, by the adatom separations shown by geometrical arguments: an $N=6$ NT leads to no overlap of potentials due to overlap of H_2 along the diagonal for $d>2$ Å. Similarly, when $N=12$, the diagonal nearest-neighbor distance becomes repulsive only for $d>3.2$ Å. Thus the $N=12$ diameter is able to accommodate the optimal H_2-C distance without overlap of H_2-H_2 neighbors along the diagonal. As R is increased, H_2 separations along the diagonal begin to lead to overlap of the H_2 potential. As the striped phase has no diagonal H_2-H_2 placements, the striped phase has the lowest energy for cases of intermediate R values, $12\leqslant N<39$. For larger R ($N>39$), as the radial H_2 distances approach the hard-core spacing, the $\sqrt{3}$ phase becomes stable. For such large R, the nearest-neighbor distances approach the spacing on the basal plane of graphite; indeed, the $\sqrt{3}$ phase is that observed experimentally for graphite.

Since these calculations are classical, one might wonder how sensitive the predictions are to this approximation. In fact, the surface-normal contribution to the quantum zero-point energy E_{zp} derived from these potentials is quite large, similar in magnitude to that found for H_2 on graphite ($E_{zp}\sim110$ K).[25] The relevant point, however, is that this holding potential is the same for molecules in the two phases being compared (1×1 and $\sqrt{3}$), so that the quantum contribution due to normal motion does not contribute significantly to the *relative* cohesive energies of these phases. We must also consider the energy difference corresponding to zero-point motion parallel to the surface. That problem has not been addressed previously because no analogous phase exists on graphite, except for the $\sqrt{3}$ phase, but we can make some general comments about it. The first is based on the problem that has been solved, the spectrum of commensurate H_2 on graphite. There, to lowest approximation, the zone-center phonon energy represents the zero-point vibrational energy (parallel to the surface) of a single molecule. That energy (47 K) has been calculated and measured experimentally with neutron scattering.[26,27] This value provides a crude estimate of the lateral vibrational energy on the nanotube. We surmise that this number will be reduced somewhat on the tube, relative to its value on the flat surface, because the potential energy corrugation is somewhat smaller outside of the nanotube. In any case, in spite of the magnitude of this energy, we do not expect that this energy contribution will

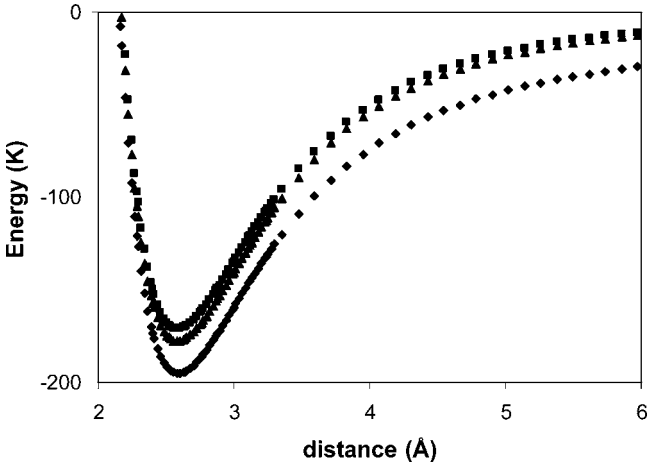

FIG. 5. Adsorption energy of He as a function of d, for the case $N=18$. Curves represent results for the 1×1 phase (diamonds), the $\sqrt{3}$ phase (squares) and the striped phase (triangles).

alter the balance between the two alternative phases significantly.

The calculated behavior of He shifts the stability regions for the various phases (Figs. 5 and 6). Unlike H_2, for He the ordering of the energies does not change within the initial range explored, $(6\leqslant N\leqslant 21)$, and the uniform result within this range is $E_{\sqrt{3}}>E_{\text{striped}}>E_{1\times1}$. Exploring larger nanotubes shows that the striped phase becomes the most stable phase at $N=54$. Thus, the 1×1 phase is predicted to be stable for nanotubes studied in the laboratory. The geometrical nearest-neighbor argument alone does not fully predict the phase stability behavior, as geometrical considerations would predict that the 1×1 phase became unstable at $N\sim45$. A transition to the $\sqrt{3}$ phase was not observed in the energy simulations up to $N=90$. The geometrical argument [Eq. (1)] predicts that the radial nearest-neighbor distance of the stripe phase becomes less than σ for He-He interactions only for $N>200$. This estimate suggests the $\sqrt{3}$ phase will become stable only for $R>78$ Å, and this is the phase observed on graphite.

The case of Ne is depicted in Fig. 7. For $N\leqslant18$, the

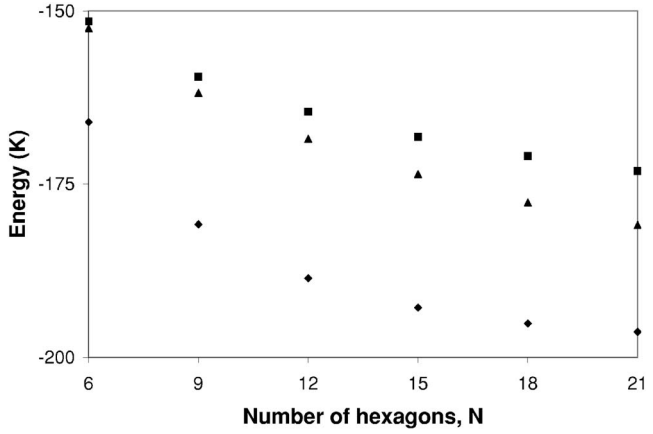

FIG. 6. Adsorption energy of He vs N. Notation is the same as in Fig. 4.

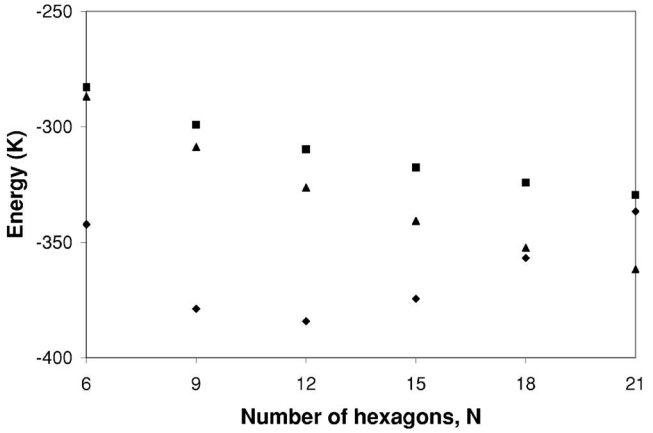

FIG. 7. Adsorption energy of Ne as a function of N for the 1×1 phase (diamonds), $\sqrt{3}$ phase (squares), and striped phase (triangles).

1×1 phase is stable, whereas the striped phase is stable for intermediate N $(18<N<60)$. The $\sqrt{3}$ phase becomes stable at $N=63$. The results are similar to the behavior observed for H_2, with a variation in the radius for the phase transition. Again, one might attribute this transition radius to the values of the gas-gas hard-core parameter (i.e., σ values are 2.928, 2.749 and 2.556 Å for H_2, Ne, and He, respectively), but the geometrical consideration predicts a phase transition from 1×1 to striped at $N\sim18$, whereas the full calculation shows the phase transition at $N=21$. At $N=18$, the energy of neon's striped phase becomes virtually identical to that of the 1×1 phase. The ground state of Ne on planar graphite is different from all of these structures; it corresponds to a $\sqrt{7}\times\sqrt{7}R19.1°$ commensurate phase, with four Ne atoms in the basis.[19,28,29] Analogous high-order commensurate phases may well occur on nanotubes, but a search for such possibilities is beyond the scope of the present study.

The behavior, shown in Figs. 8 and 9, of Ar on NTs manifests the progression toward a relatively favorable striped phase (compared to 1×1) as the σ parameter increases

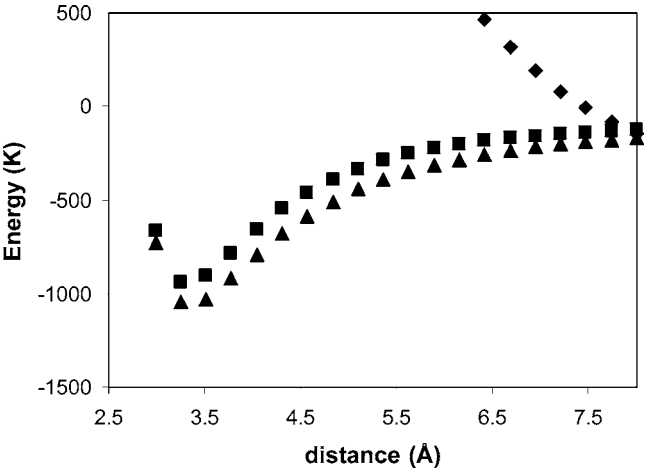

FIG. 8. Adsorption energy of Ar as a function of d for the case of $N=18$. Curves represent results for the 1×1 phase (diamonds), the $\sqrt{3}$ phase (squares), and the striped phase (triangles).

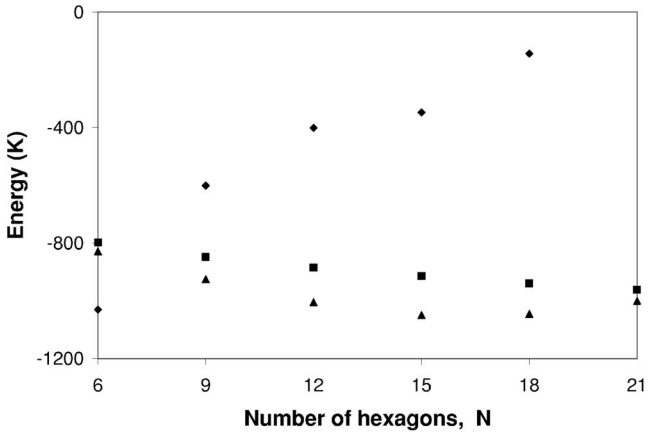

FIG. 9. Adsorption energy of Ar as a function of N for the 1×1 phase (diamonds), $\sqrt{3}$ phase (squares), and striped phase (triangles).

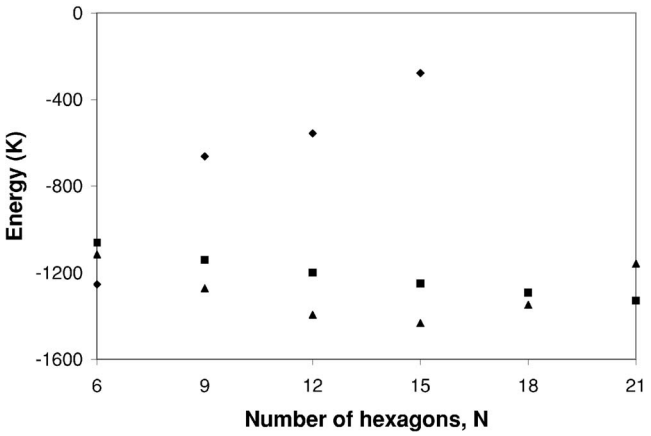

FIG. 11. Adsorption energy of Kr as a function of N for $\sqrt{3}$ phase (squares) and striped phase (triangles). The 1×1 phase (diamonds) is not favored in the range of N shown.

$(\sigma_{Ar}/\sigma_{He}\sim1.38)$. For $9\leqslant N\leqslant21$, the striped phase is favored for Ar. For smaller $N<9$, the 1×1 has lower energy, while for larger N the $\sqrt{3}$ phase is stable. A nearly identical dependence of structure on N is found for Kr, for which the results are shown in Figs. 10 and 11. The only difference is a detail: the phase of Kr first becomes stable at $N=21$.

The Xe behavior continues the trend associated with increasing atomic size (Figs. 12 and 13). For $N\leqslant12$ the striped phase is energetically favored, while for larger N the $\sqrt{3}$ phase is stable. For planar graphite, in fact, the $\sqrt{3}$ phase is close to stability, as compared with the incommensurate phase (which is not considered here). The different behavior in the NT case is, of course, due to the curvature, favoring the $\sqrt{3}$ phase, which is less compressed than on graphite.

III. SUMMARY AND DISCUSSION

Figure 14 presents a summary of our results for the various gases studied. There is a clear trend consistent with the geometrical argument mentioned in Sec. II. Specifically, increasing N favors less dense phases; however, at a given value of N, the large (small) diameter gases "prefer" less (more) dense phases.

In general, there is a remarkably close correspondence between predictions based on the geometrical argument of Sec. II A and the predictions based on the full energy calculations, shown in Fig. 14. There is, however, a small discrepancy with respect to the relative stability of striped and $\sqrt{3}$ phases. In particular, the upper N limit to the domain of striped phase stability is predicted by the geometrical argument to be slightly larger than is found in the energy calculation.

The present calculations have been carried out for gases adsorbed on the outside of isolated individual nanotubes. While individual tubes are often found in laboratory samples of nanotubes, these are usually assembled to form nanotube bundles and/or deposited on surfaces. Such systems may be studied theoretically by the techniques used here and are expected to result in qualitatively similar phenomena. Indeed, our group and many other groups have studied adsorption inside single nanotubes and inside and outside nanotube bundles.

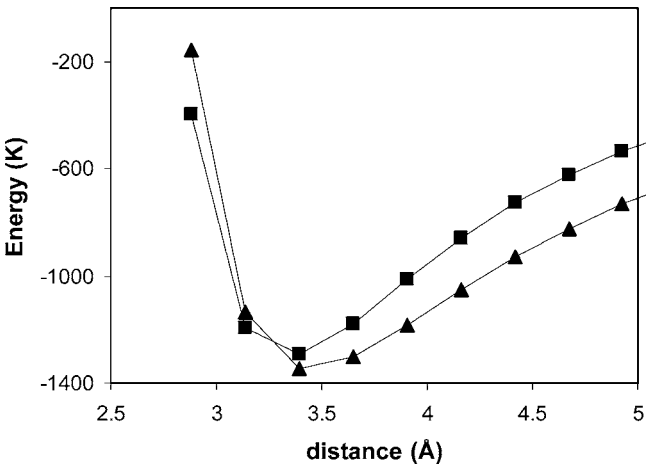

FIG. 10. Adsorption energy for Kr, for various phases, with $N=18$, for the $\sqrt{3}$ phase (squares) and striped phase (triangles). The energy of the 1×1 phase is far off scale ($E>500$ K).

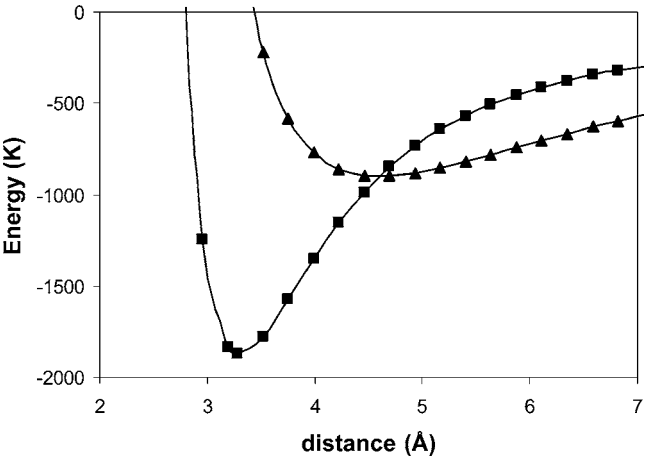

FIG. 12. Adsorption energy for Xe, for various phases, with $N=18$, for the $\sqrt{3}$ phase (squares) and striped phase (triangles). The 1×1 phase is not shown ($E>10\,000$ K).

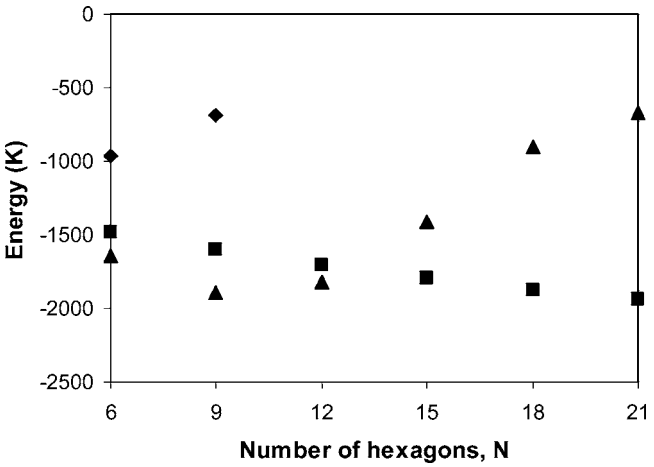

FIG. 13. Adsorption energy of Xe as a function of N for $\sqrt{3}$ phase (squares) and striped phase (triangles). The 1×1 phase (diamonds) is repulsive for $N>9$.

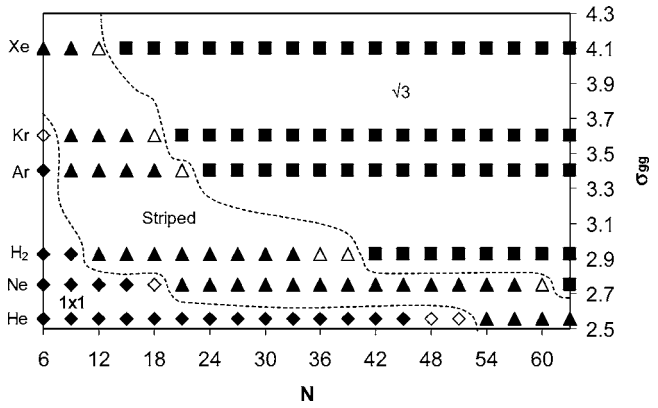

FIG. 14. Phases for various gases, with specified σ_{gg}, on NTs of varying N, as predicted by energy calculations. Symbols represent the 1×1 phase (diamonds), the striped phase (triangles), and the $\sqrt{3}$ phase (squares). The dotted lines (drawn to guide the eye) delineate the phases predicted from the energy calculations. The hollow points represent cases where the prediction based on geometry (discussed in the text) does not agree with that from the energy calculation.

The present study predicts the existence of various commensurate phases at temperature $T=0$. At nonzero T, rigorous theorems forbid the existence of such well-defined phases, insofar as the system is 1D from a phase transition perspective. Studies of the thermal properties of similar phases within nanotubes have shown, however, that "quasi-transitions" occur. These correspond to the appearance of commensurate regions of gas persisting over extended correlation lengths. Thermal signatures of these transitions are qualitatively similar to those of true transitions, although no singularities occur.[30] Similar behavior is to be expected from the appearance of the commensurate phases discussed here. In future work, we intend to explore these proposed transitions with computer simulations, a technique that has been applied extensively to study adsorption on NTs.

An alternative experimental probe of the phases discussed in this paper is Raman spectroscopy. This offers the potential to see the breathing mode of the adsorbed phase. We shall present results of such a study in the future.[31]

ACKNOWLEDGMENTS

This research has been supported by the National Science Foundation (Grant No. NSF DMR-0505160) and the Petroleum Research Fund of the American Chemical Society (Grant No. 43431-G10). We are grateful to Susana Hernández for helpful discussions and comments concerning this manuscript and to Erik Schaible and Nikola Grozdanic for assistance in coding the program.

[1] *Phase Transitions in Surface Films*, edited by H. Taub, G. Torzo, H. J. Lauter, and S. C. Fain, (Plenum, New York, 1991).
[2] O. E. Vilches, Annu. Rev. Phys. Chem. **31**, 463 (1980).
[3] *Adsorption by Carbons*, edited by Juan M. D. Tascon (Elsevier Science Publishing, Amsterdam, 2006).
[4] N. D. Shrimpton, M. W. Cole, W. A. Steele, and M. H. W. Chan, in *Surface Properties of Layered Structures*, edited by G. Benedek (Kluwer Academic, Dordrecht, the Netherlands, 1992), pp. 219–260; H. Godfrin and H. J. Lauter, in *Progress in Low Temperature Physics*, edited by W. P. Halperin (Elsevier, Amsterdam, 1995), Vol. XIV, p. 213.
[5] L. W. Bruch, M. W. Cole, and E. Zaremba, *Physical Adsorption: Forces and Phenomena* (Oxford University Press, Oxford, 1997).
[6] L. Onsager, Phys. Rev. **65**, 117 (1944); C. N. Yang, *ibid.* **85**, 808 (1952).
[7] H. K. Kim and M. H. W. Chan, Phys. Rev. Lett. **53**, 170 (1984).
[8] J. G. Dash, M. Schick, and O. E. Vilches, Surf. Sci. **299/300**, 405 (1994).
[9] H. Wiechert, Physica B **169**, 144 (1991).
[10] D. M. Butler, J. A. Litzinger, and G. A. Stewart, Phys. Rev. Lett. **44**, 466 (1980); A. D. Migone, M. H. W. Chan, K. J. Niskanen, and R. B. Griffiths, J. Phys. C **16**, L1115 (1983).
[11] M. Bretz, Phys. Rev. Lett. **38**, 501 (1977).
[12] B. Nienhuis, A. N. Berker, E. K. Riedel, and M. Schick, Phys. Rev. Lett. **43**, 737 (1979).
[13] C. K. W. Adu, G. U. Sumanasekera, B. K. Pradhan, H. E. Romero, and P. C. Eklund, Chem. Phys. Lett. **337**, 31 (2001).
[14] A. C. Dillon and M. J. Heben, Appl. Phys. A: Mater. Sci. Process. **72**, 133 (2001); T. Wilson *et al.*, J. Low Temp. Phys. **126**, 403 (2002); M. Hirscher and M. Becker, J. Nanosci. Nanotechnol. **3**, 3 (2003); A. D. Migone and S. Talapatra, in *Encyclopedia of Nanoscience and Nanotechnology*, edited by H. S. Naiwa (American Scientific, Los Angeles, 2004), Vol. 4, p. 749; S. B. Sinnott and R. Andrews, CRC Crit. Rev. Solid State Mater. Sci. **26**, 145 (2001); R. H. Baughman, A. A. Zakhidov, and W. A. de Heer, Science **297**, 787 (2002); S. R. Challa, D. S. Sholl, and J. K. Johnson, J. Chem. Phys. **116**, 814 (2002); R. A. Trasca, M.

K. Kostov, and M. W. Cole, Phys. Rev. B **67**, 035410 (2003).
[15] Oleg Byl, Jin-Chen Liu, Yang Wang, Wai-Leung Yim, J. Karl Johnson, and John T. Yates, Jr., J. Am. Chem. Soc. **128**, 12090 (2006); Lucyna Firlej and Bogdan Kuchta, Colloids Surf., A **241**, 149 (2004).
[16] G. Stan and M. W. Cole, J. Low Temp. Phys. **110**, 539 (1998).
[17] C. G. Shaw and S. C. Fain, Jr., Surf. Sci. **83**, 1 (1979); **91**, L1 (1980).
[18] M. M. Calbi, S. M. Gatica, M. J. Bojan, and M. W. Cole, Phys. Rev. E **66**, 061107 (2002); A. Šiber, Phys. Rev. B **68**, 033406 (2003); V. V. Simonyan *et al.*, J. Chem. Phys. **114**, 4180 (2001). V. V. Simonyan, J. K. Johnson, A. Kuznetsova, and J. T. Yates, Jr. [*ibid.* **114**, 4180 (2001)] observed no such phases in their finite-T study.
[19] X. Yang and J. Ni, Phys. Rev. B **69**, 125419 (2004).
[20] W. E. Carlos and M. W. Cole, Surf. Sci. **91**, 339 (1980); J. M. Phillips and L. W. Bruch, J. Chem. Phys. **79**, 6282 (1983).
[21] D. M. Ceperley, Rev. Mod. Phys. **67**, 279 (1995); E. S. Hernández and J. Navarro, in *Microscopic Approaches to Quantum Liquids in Confined Geometries*, edited by E. Krotscheck and J. Navarro (World Singapore, Singapore, 2002), p. 147–213.
[22] M. Boninsegni and S. Moroni, J. Low Temp. Phys. **118**, 1 (2000).
[23] R. S. Berry, S. A. Rice, and J. Ross, *Physical Chemistry* (Wiley, New York, 1980), Table 21.13.
[24] Such combining rules are not always reliable; see G. Scoles, Int. J. Quantum Chem. **24**, 475 (1990). However, in the present case they use empirical C interaction parameters, derived from adsorption experiments, so they are relatively trustworthy and therefore are employed conventionally.
[25] L. Mattera *et al.*, Surf. Sci. **93**, 515 (1980); G. Vidali, in *Physical Adsorption: Forces and Phenomena* (Ref. 5), Fig. 2.8.
[26] A. D. Novaco, Phys. Rev. B **46**, 8178 (1992).
[27] H. J. Lauter, V. L. P. Frank, H. Taub, and P. Leiderer, Physica B **165/166**, 611 (1990).
[28] G. B. Huff and J. G. Dash, J. Low Temp. Phys. **24**, 155 (1976).
[29] L. W. Bruch, J. M. Phillips, and X.-Z. Ni, Surf. Sci. **136**, 361 (1984).
[30] R. A. Trasca, M. M. Calbi, M. W. Cole, and J. L. Riccardo, Phys. Rev. E **69**, 011605 (2004).
[31] S. M. Gatica, A. D. Lueking, M. W. Cole, and G. D. Mahan, (unpublished).